Available online at www.sciencedirect.com
ScienceDirect
Chinese Journal of Natural Medicines 2021, **19**(5): 351-363
doi: 10.1016/S1875-5364(21)60033-X
Chinese Journal of Natural Medicines

•Research article•

Ziyuglycoside II inhibits the growth of digestive system cancer cells through multiple mechanisms

ZHONG Ying[1], LI Xiao-Yu[1], ZHOU Fei[2], CAI Ya-Jie[2], SUN Rong[1*], LIU Run-Ping[2*]

[1] *The Second Hospital, Cheeloo College of Medicine, Shandong University, Jinan 250033, China;*
[2] *School of Chinese Materia Medica, Beijing University of Chinese Medicine, Beijing 100029, China*

Available online 20 May, 2021

[ABSTRACT] Digestive system cancers, including liver, gastric, colon, esophageal and pancreatic cancers, are the leading cause of cancers with high morbidity and mortality, and the question of their clinical treatment is still open. Previous studies have indicated that Ziyuglycoside II (ZYG II), the major bioactive ingredient extract from *Sanguisorba officinalis* L., significantly inhibits the growth of various cancer cells. However, the selective anti-tumor effects of ZYG II against digestive system cancers are not systemically investigated. In this study, we reported the anti-cancer effect of ZYG II on esophageal cancer cells (OE21), cholangiocarcinoma cells (HuCCT1), gastric cancer cells (BGC-823), liver cancer cells (HepG2), human colonic cancer cells (HCT116), and pancreatic cancer cells (PANC-1). We also found that ZYG II induced cell cycle arrest, oxidative stress and mitochondrial apoptosis. Network pharmacology analysis suggested that UBC, EGFR and IKBKG are predicted targets of ZYG II. EGFR signaling was suggested as the critical pathway underlying the anti-cancer effects of ZYG II and both docking simulation and western blot analysis demonstrated that ZYG II was a potential EGFR inhibitor. Furthermore, our results showed synergistic inhibitory effects of ZYG II and chemotherapy 5-FU on the growth of cancer cells. In summary, ZYG II are effective anti-tumor agents against digestive cancers. Further systemic evaluation of the anti-cancer activities *in vitro* and *in vivo* and characterization of underlying mechanism will promote the development of novel supplementary therapeutic strategies based on ZYG II for the treatment of digestive system cancers.

[KEY WORDS] Ziyuglycoside II; Digestive system cancers; Network pharmacology; EGFR pathway
[CLC Number] R965 **[Document code]** A **[Article ID]** 2095-6975(2021)05-0351-13

Introduction

Digestive system neoplasms, including esophageal cancer (EC), gastric cancer (GC), hepatocellular carcinoma (HCC), cholangiocarcinoma (CCA), pancreatic cancer (PC) and colorectal cancer (CRC), are accounting for more than one-quarter of newly diagnosed cancer cases, and have become the second leading cause of cancer-related death [1, 2]. The remarkable rise in the incidence of digestive cancers during the past decades has been ascribed to the continuous environmental pollution, diet-related obesity, alcohol consumption and also active tobacco smoking [1]. Although recent progresses in the development of anti-cancer therapies, including radiotherapy, target therapy and immunotherapy, have greatly contributed to the large declines in mortality rate and to the prolonged survival time of various cancers, the 5-year survival rate for digestive cancers is still low, specifically, only about 64.9% in colorectal cancers, about 30.0% in gastric cancers, about 17.8% in esophagus cancers, about 17.2% in liver cancer and about 7.2% in pancreatic cancer, about 16.5% in biliary cancer, which is compiled by National Cancer Institute (https://seer.cancer.gov). Poor survival rates for these cancers are potentially attributed to late diagnosis, inherent resistance to chemotherapy and a lack of effective target therapies. Therefore, the discovery and evaluation of novel anti-cancer candidates or complementary approaches facilitating the efficacy of current chemotherapies are urgently required for the treatment of digestive cancers.

Sanguisorba officinalis L., a member of rosaceous family, is a widely prescribed Traditional Chinese Medicine herbal product, exerting various pharmacological effects, including “heat ” clearance, detoxification, hemostasis, antidiarrheal and inhibitory effects against various of pathogenic

[Received on] 03-Aug.-2020
[Research funding] This work was supported by the grants from Beijing University of Chinese Medicine (Nos. 1000041510166 and 2020-JYB-ZDGG-038), the National Natural Science Foundation of China (No. 81773997), the Shandong Province Key Research Program (2016ZDJS07A21 and 2017CXGC1301). SUN Rong is supported by research fund "Traditional Chinese medicine pharmacology and toxicology expert (No. ts201511107)" from Taishan Scholar Project of Shandong Provinceince.
[*]**Corresponding author]** E-mail: sunrong@sdu.edu.cn (SUN Rong); liurunping@bucm.edu.cn (LIU Run-Ping)
These authors have no conflict of interest to declare.

microorganisms [3, 4]. The major bioactive ingredients of *Sanguisorba officinalis* L. are triterpenoid saponins, tannins and flavonoids. Ziyuglycoside (ZYGs) are triterpenoid saponins isolated and identified from *Sanguisorba officinalis* L., including Ziyuglycoside I (ZYG I) and ZYG II (Fig. 1A) [5]. Emerging studies have suggested the potential therapeutic effects of ZYG-I against leukopenia and cancers [6-8]. Similar to ZYG I, ZYG II has also attracted increasing attentions for its anti-cancer activities. Recent studies indicated that ZYG II inhibited breast cancer metastasis by targeting Src/EGFR-dependent ITGB4/FAK signaling, and ROS/JNK pathway [9]. It is also testified the function of anti-angiogenic effect of ZYG II, which is closely associated with cancer progression [10]. In the researches of digestive cancers, it has been reported that ZYG II triggered mitochondria-dependent apoptosis in gastric cancer cells and induced both caspases-dependent and caspases-independent cell death in human colon cancer cells. A most recent study further suggested that ZYG II exerts antiproliferative and anti-metastatic effects on hepatocellular carcinoma cells [11-15]. Nevertheless, the comparison of anti-cancer efficacy of ZYG II against different types of digestive cancers, especially cholangiocarcinoma, esophagus cancers, and pancreatic cancers, is still missing and the underlying mechanisms are still unknown.

In the present study, we evaluated the effects of ZYG II on the growth of various digestive cancer cell lines, including HCC, CCA, EC, PC, GC and CC, and further explore the potential mechanisms using HCC cell line HepG2. We also aimed to elucidate the plausible molecular targets of ZYG II by employing network pharmacology and molecular modeling approaches. Furthermore, the synergetic effects of ZYG II and conventional chemotherapy 5-Fu on the proliferation of HepG2 were investigated. The results suggested that ZYGII significantly induced digestive cancers cells apoptosis and facilitates the anti-cancer effects of 5-Fu by regulating cell cycle progression, mediating oxidative stress, and interrupting EGFR signaling.

Materials and Methods

Materials

ZYG II (purity > 99%, MW: 604.8) was purchased from National Institute for the Control of Pharmaceutical and Biological Products (Beijing, China). 5-FU (10 mL: 0.25 g) was purchased from XuDong HaiPu Pharmaceutical Company (Shanghai, China). Fetal calf serum (FCS), penicillin G, streptomycin, and amphotericin B were obtained from GIBCO BRL (Gaithersburg, MD), dimethyl sulfoxide (DMSO), Dulbecco's modified Eagle's medium (DMEM)

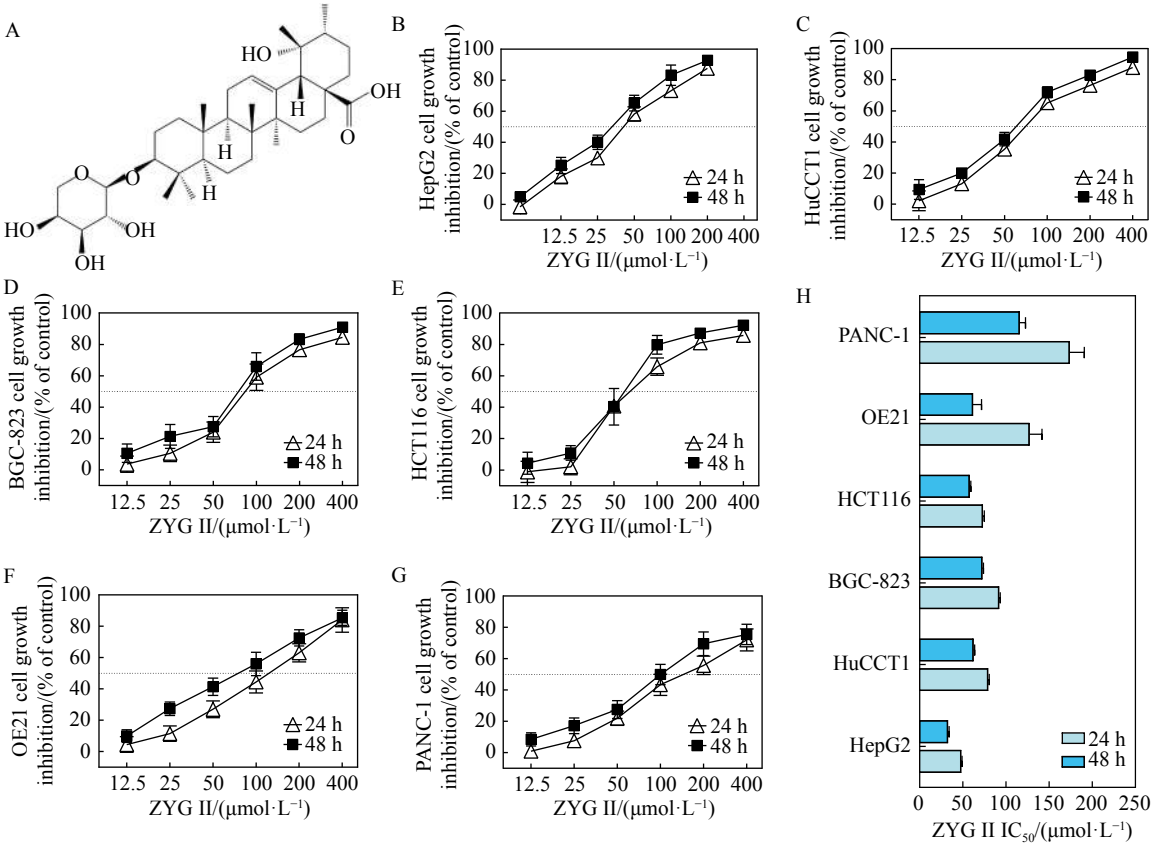

Fig. 1 ZYG II inhibits the proliferation of digestive cancer cells. (A) the structure of ZYG II. (B–G) HepG2 cells (B), HuCCT1cells (C), BGC-823 cells (D), HCT116 cells (E), OE21 cells (F) and PANC-1 cells (G) were treated with various concentrations of ZYG II (12.5, 25, 50, 100, 200, and 400 μmol·L^{-1}) for 24 h and 48 h. At the end of experiment, cell availability was determined by CCK-8 assay. (H) The IC_{50} of ZYG II in different cell lines are calculated and are shown as mean ± SEM

and ribonuclease (RNase)were purchased from Sigma Chemical (St.Louis, MO). Annexin V-FITC and PI double staining kit was obtained from BD Biosciences (CA, USA), Enhanced Cell Counting Kit-8 (CCK-8), Ros assay kit and Mitochondrial membrane potential assay kit with JC-1was acquired from Beyotime Institute of Biotechnology (Hangzhou, China). The information about the antibodies used in this study shows as following: Cleaved Caspase-3 (Asp175) Antibody (Trevigen, MD, USA), PARP (Poly(ADP-ribose) Polymerase) Host: Mouse (Kamiya, PA, USA), Anti-GAPDH Monoclonal Antibody, Bcl-2, Bax, and the HRP conjugated goat anti mouse/rabbit secondary antibodies(Santa Cruz, CA, USA).

Cell lines and cell culture

Liver cancer cell line (HepG2), human cholangiocarcinoma cell line (HuCCT1), gastric cancer cell line (BGC-823), human colonic cancer cell line (HCT116), esophageal cancer cell line (OE21), pancreatic cancer cell line (PANC-1), obtained from Shanghai Institutes for Biological Sciences, were used in this study. All the cell lines were maintained at 37 °C in a humidified atmosphere containing 5% CO_2.

Cell proliferation assay to assess the effect of ZYG II on cell growth

Cells (1×10^4 cells/well) were seeded in 96-well culture plates. After 24 h incubation, hepG2 cells were treated with various concentrations of ZYG II (5.75, 12.5, 25, 50, 100, and 200 μmol·L^{-1}) for 24 h and 48 h respectively, while HuCCT1, BGC-823, HCT116, OE21 and PANC-1cells were treated with concentrations of 12, 25, 50, 100, 200, and 400 μmol·L^{-1}. At the end of incubation, cell proliferation was measured by CCK-8 kit. Briefly, for CCK-8 assay, 10 μL CCk-8 stock solution was added to each well to incubate for 1 h at 37 °C, then absorbance was measured at 450 nm with a Microplate reader (Bio-Rad, CA, USA), and IC50 was calculated. All data were expressed as mean ± SD of six experiments and each experiment included triplicate repeats.

Measurement of cell apoptosis

Apoptosis of cells was examined by double staining with Annexin V-FITC and PI. After treatment with various concentrations of ZYG II (0, 25, 50 and 100 μmol·L^{-1}) for 24 h, cells were washed twice with ice-cold PBS and re-suspended in 300 μL binding buffer (Annexin V-FITC kit, Becton-Dicknson, CA, USA) containing 10 μL of Annexin V-FITC stock and 10 μL of PI. After incubation for 15 min at room temperature in dark, the samples were then analyzed by flow cytometry. The Annexin V^+/PI^- cells were considered as apoptotic cells and the percentage of which was calculated by Cell Quest software (Becton-Dickinson, CA, USA)ton-Dickinson, CA, USA)

Western blotting analysis

For western blotting analysis, approximately 1×10^6 cells were collected and lysed in ice-cold RIPA buffer. Protein concentration was determined by the Bradford method (Bradford, 1976). Cell lysates were electrophoresed on a 15% SDS polyacrylamide gel and transferred onto PVDF membrane. After blocking with 5% bovine serum albumin (BSA) in the mixture of Tris-Buffered Saline and Tween-20 (TBST) for 1 h, membranes were incubated with primary antibody overnight and followed by incubation with secondary antibody for 1 h at room temperature. Protein bands were visualized using the ECL assay kit (Beyotime, Hangzhou, China). The antibodies used were against Bcl-2, Bax, Cleaved-Caspase3, Cleaved-PARP, *β*-ACTIN.

Cell cycle distribution

Cells (1×10^6 cells/well) were seeded in 6-well plates and incubated overnight. Then the cells were serum starved for 24 h to synchronize into the GO phase of cell cycle. Synchronous populations of cells were incubated with various concentrations of ZYG II (0, 25, 50 and 100 μmol·L^{-1}) for 24 h, washed twice with ice-cold PBS and then centrifuged. The pellet was fixed in 75% (*V*/*V*) ethanol for 1 h at 4 °C, washed once with ice-cold PBS and then suspended in cold PBS supplied with propidiumiodide (PI) solution (50 pg·mL^{-1}) as well as ribonuclease A (RNase A) (0.7 mg·mL^{-1}) for 30 min in the dark. Cell cycle distribution was assessed using flow cytometer (Becton-Dickinson, CA, USA).

Measurement of reactive oxygen species (ROS)

Cells (1×10^4 cells/well) were seeded in 96-well culture plates. After 24 h incubation, hepG_2 cells were treated with various concentrations of ZYG II (10, 20, 40 μmol·L^{-1}) for 24 h. Cells were suspend in the diluted DCFH-DA solution whose concentration was 10 μmol·L^{-1}, incubated at 37 °C for 20 min, then washed three times with serum-free cell culture medium.The level of ROS was then analyzed by flow cytometry.

Measurement of mitochondrial membrane potential (MMP)

The level of MMP was determined by flow cytometry using mitochondrial membrane potential assay kit with JC-1. At higher membrane potentials, JC-1 monomers convert to J-aggregates that emit a red light (590 nm) following excitation by light (585 nm). Fluorescence was monitored at wavelengths of 490 nm (excitation)/530 nm (emission). Changes in the ratio between the measurement at wavelengths of 590 nm and 585 nm fluorescence intensities indicated the alternation of MMP level. The level of MMP was then analyzed by flow cytometry.

Collecting compound-disease common targets

The known therapeutic and mechanism targets of drugs used in of HCC, GC, CLC, CRC EC and PC were acquired from Comparative Toxicogenomics Database (http://ctdbase.org/). Using drug–target interactions mentioned in Drug Bank to selected for the treatment target of HCC, GC, CLC, CRC, EC and PC and whose targets are human genes/proteins. An updated integrated pharmacophore matching platform with statistical method for potential target identification tool PharmMapper Server (http://lilab.ecust.edu.cn/pharmmapper/, version 2017), effective for quick identification of all molecules with structure similarities, was used to identify potential target candidates for the given probe small molecules (drugs, natural products, or other newly discovered com-

pounds with binding targets unidentified). 2D and 3D Chemical structure of ZYG II were obtain from Pubchem Compound (https://www.ncbi.nlm.nih.gov/pubmed), and Then, the therapeutic targets of ZYG II, obtained from the PharmMapper Server, were considered as putative targets of ZYG II. To improve the reliability of the target prediction results, only drugs with a high structural similarity score (> 0.80, moderately similar to very similar) were selected.

Construction and analysis of PPI network

Putative ZYG II target-known therapeutic targets of typical digestive cancer, including HCC, GC, CLC, CRC, EC and PC, network and putative ZYG II target networks were constructed. All the target genes were imported into the BisoGenet,which is a big database in Cytoscape (version 3.6.1; https://www.cytoscape.org/) software, to create a Protein-protein interaction (PPI) network. The interaction proteins of ZYG II and one choice cancer will be merged and choice by the median scores of betweeness, clonuness, degree, eigenvetor, LAC, network in CytoNCA to create a core network. The node size and color was used to reflect the number of combined targets (degree), and the line size and color will reflect the the combines scores with each node.

GO and KEGG pathway enrichment analysis

The biological process, molecular function, pathway of Genes and Genomes (KEGG) database (https://www.kegg.jp/) pathway enrichment analysis was using the CluGO in Cytoscape (https://www.cytoscape.org/). In this research, KEGG pathway enrichment analyses were performed using the *P* value less than 0.05 was employed for further analysis. In this research, GO functional annotation were performed in Cytoscape, choosing most probable pathway whose *P*-value scores were in ascending order.

Molecular docking simulation

Molecular modeling was performed using Sybyl-x 2.0 software from Tripos Inc. (St. Louis, MO). The 3D structures of the compound ZYG II and positive drug Sorafenib was downloaded from the ZINC database. The crystal structure the EGFR kinase (PDB ID: 2GS6), HER2 (PDB ID: 3PP0) and Vegfr2 (PDB ID: 2OH4) was directly downloaded from the RCSB protein data bank. The protein structure was optimized for docking as follows: H atoms were added, all water molecules were removed from the crystal structure, and the bound ligand was extracted and then prepared with the protein preparation module using default parameters, and the program generated the protomol in the active site of protein with a threshold of 0.5 and bloat set of 1 around the embedded molecule. The Surflex-Dock (SFXC) docking mode was employed to fit the ligands and protein and the Surflex-Dock scores were obtained.

Western blotting analysis for EGFR

Cells (1×10^4 cells/well) were seeded in 96-well culture plates. After 24 h incubation, $HepG_2$ cells were treated with ZYG II (20 μmol·L^{-1}) for 1, 2, 6, 12, 24 h, and treated with indicated concentrations of ZYG II (10, 20, 40 μmol·L^{-1}) for 24 h respectively. For western blotting analysis, approximately 1×10^6 cells were collected and lysed in ice-cold RIPA buffer. Protein concentration was determined by the Bradford method (Bradford, 1976). Cell lysates were electrophoresed on a 15% SDS polyacrylamide gel and transferred onto PVDF membrane. After blocking with 5% bovine serum albumin (BSA) in the mixture of Tris-Buffered Saline and Tween-20 (TBST) for 1 h, membranes were incubated with primary antibody overnight and followed by incubation with secondary antibody for 1 h at room temperature. Protein bands were visualized using the ECL assay kit (Beyotime, Hangzhou, China). The antibodies used were against EGFR and ERK1/2. After choose the best time for ZYG II, Cells (1×10^4 cells/well) were seeded in 96-well culture plates. After 24 h incubation, HepG2 cells treated with indicated concentrations of ZYG II (10, 20, 40 μmol·L^{-1}) for 1 h. EGF (10 ng·mL^{-1}) was given after that for 1 h. Repeat the above western blotting analysis.

Drug combination of ZYG II and 5-FU

To assess the effect of ZYG II on cell growth, cells (1 × 104 cells/well) were seeded in 96-well culture plates. After 24 h incubation, hepG2 cells were treated with various concentrations of 5-FU (12.5, 25, 50, 100, 200 and 400 μmol·L^{-1}) for 24 hours. Others are treated by various concentrations of ZYG II (10, 20 and 40 μmol·L^{-1}), in the meantime, each concentration of ZYG II will be combined with each concentrations of 5-FU (12.5, 25, 50, 100, 200 and 400 μmol·L^{-1}). At the end of incubation, cell proliferation was measured by CCK-8 kit. Briefly, for CCK-8 assay, 10 μL CCk-8 stock solution was added to each well to incubate for 1 h at 37 °C, then absorbance was measured at 450 nm with an Microplate reader (Bio-Rad, CA, USA), and IC50 was calculated. All data were expressed as mean ± SD of six experiments and each experiment included triplicate repeats. The inhibition rate will be import into the Compusyn (http://www.combosyn.com), a professional software in calculating the combination in drugs, to form the Fa-log (DRI) plot and Fa-CI plot.

Statistical analysis

Biostatistical analyses were conducted by the SPSS 16.0 software package (Chicago, IL, USA). All experiments were repeated three times. Results of multiple experiments were expressed as mean ± SD. A value of *P* value less than 0.05 was accepted as statistically significant

Result

ZYG II inhibited digestive cancer cells proliferation

Cell growth inhibition was determined by CCK-8 assay kit. As shown in Fig. 1B−1G the growth of HCC cell line HepG2, CCA cell line HuCCT1, GC cell line BGC-823, CC cell line HCT116, EC cell line OE21, and PC cell line PANC-1 was inhibited by ZYG II in a dose-dependent manner. The IC_{50} of 24 and 48 h ZYG II treatment were 48.163 and 32.880 μmol·L^{-1} for HepG2 cell line, 79.280 and 62.320 μmol·L^{-1} for HuCCT1 cell line, 91.933 and 72.860 μmol·L^{-1} for BGC-823 cell line, 73.400 and 58.067 μmol·L^{-1} for

HCT116 cell line, 127.300 and 61.767 μmol·L^{-1} for OE21 cell line, and 173.800 and 115.907 μmol·L^{-1} for PANC-1 cell line. According to Fig. 1H, the IC50 of ZYG II in HepG2 cells were significantly lower than those in other cell types, suggesting that HepG2 cells were most sensitive to ZYG II-induced anti-proliferative effects. The anti-cancer effects of ZYG II were similar in CCA, CC and GC cell lines, whereas PC and EC cell lines were potentially resistant to ZYG II treatment. The most sensitive cell line HepG2 was used to further explore the possible mechanism.

ZYG II promoted caspase-dependent apoptosis

To investigate the molecular mechanism of ZYG II-mediated cell growth arrest, apoptosis were evaluated by flow cytometric analysis detecting Annexin V and PI staining. As shown in Fig. 2A, as low as 10 μmol·L^{-1} ZYG II significantly induced both early apoptosis, as indicated by Annexin V (FL1) positive and PI negative (FL2), and late apoptosis, as indicated by double positive staining, in 11.57% ± 1.20% and 28.87% ± 1.39% of cells. ZYG II at 20 and 40 μmol·L^{-1} further dose-dependently promoted apoptosis in more than 60% and 75% of all cells, respectively. In support of the results from Annexin V-PI staining, the expressions of BAX, a pro-apoptotic protein, was dose-dependently induced by the treatment of ZYG II for 24 h, as demonstrated by Western blot in Fig. 2C and 2D. As expected, The cleaved Caspase-3 and cleaved PARP were also significantly upregulated by ZYG II, suggesting the activation of Caspase-dependent apoptotic pathways upon ZYG II challenges.

ZYG II arrested cell cycle at G0/G1 phase and induced oxidative stress

To examine the molecular mechanism of ZYG II-mediated apoptosis, cell cycle progression was assessed by flow cytometric analysis after treated with ZYG II (0, 10, 20, 40 μmol·L^{-1}) for 24 h. As shown in Fig. 3A and 3B, ZYG II induced G0/G1 phase arrest at 24 h. Specifically, when compared to the control group, 10, 20 and 40 μmol·L^{-1} ZYG II significantly increased the cell population at the G0/G1 phase from G0/G1 phase from 67.20% ± 2.69% to 68.25% ±

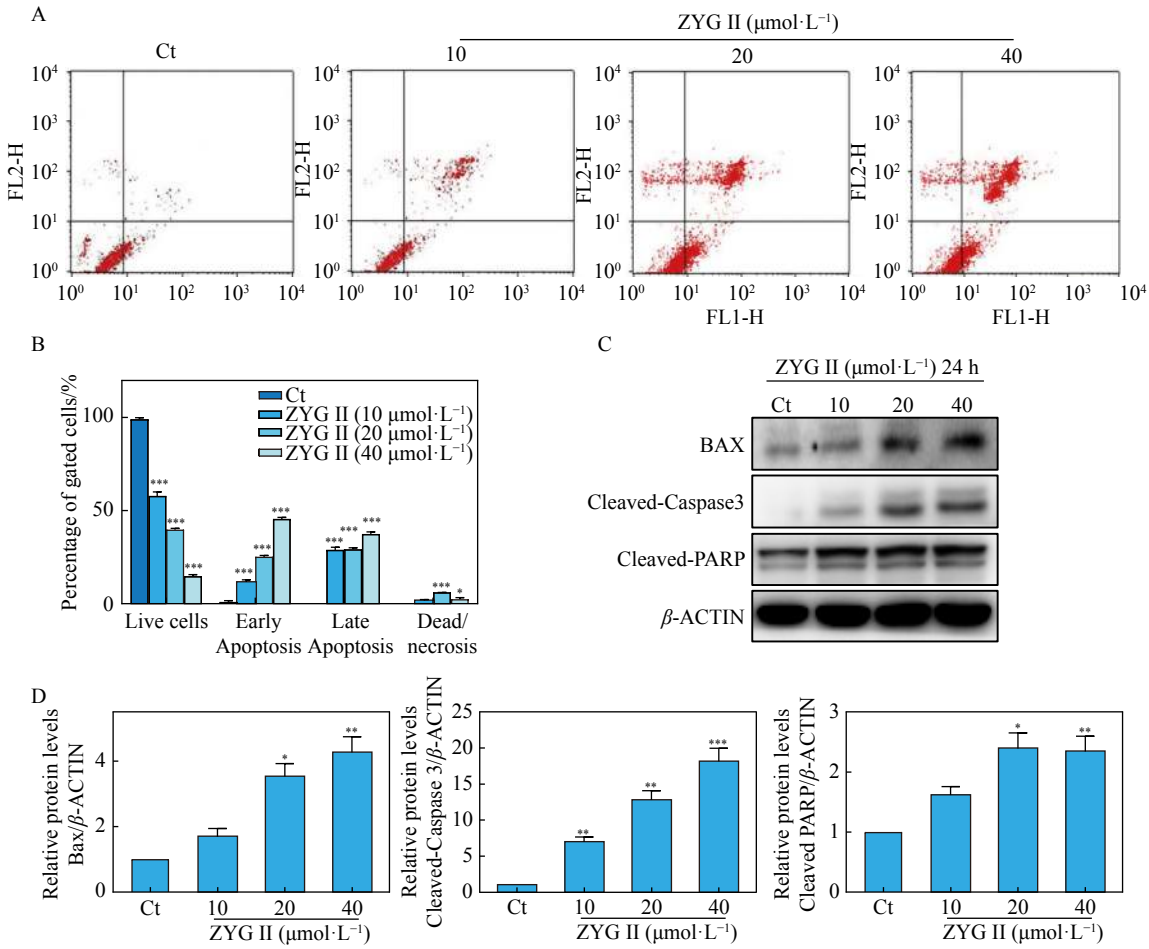

Fig. 2 ZYG II promotes apoptosis in cancer cells. (A−B) HepG2 cells were treated with ZYG II (0, 10, 20, 40 μmol·L^{-1}) for 24 h and were then analyzed by Annexin V-PI staining using flow cytometry. The percentage of live cells, early apoptotic cells, late apoptotic cells and dead cells are shown. (C) Cells were incubated with various concentrations of ZYG II for 24 h and then the expressions of cleaved-caspase 3, PARP, and BAX were assessed by western blot analysis. (D) Relative protein levels of BAX/β-ACTIN, Cleaved-Caspase3/β-ACTIN and Cleaved-PARP/β-ACTIN were analyzed. The results are expressed as the means ± SEM from three independent experiments. $^{*}P < 0.05$, $^{**}P < 0.01$, $^{***}P < 0.001$

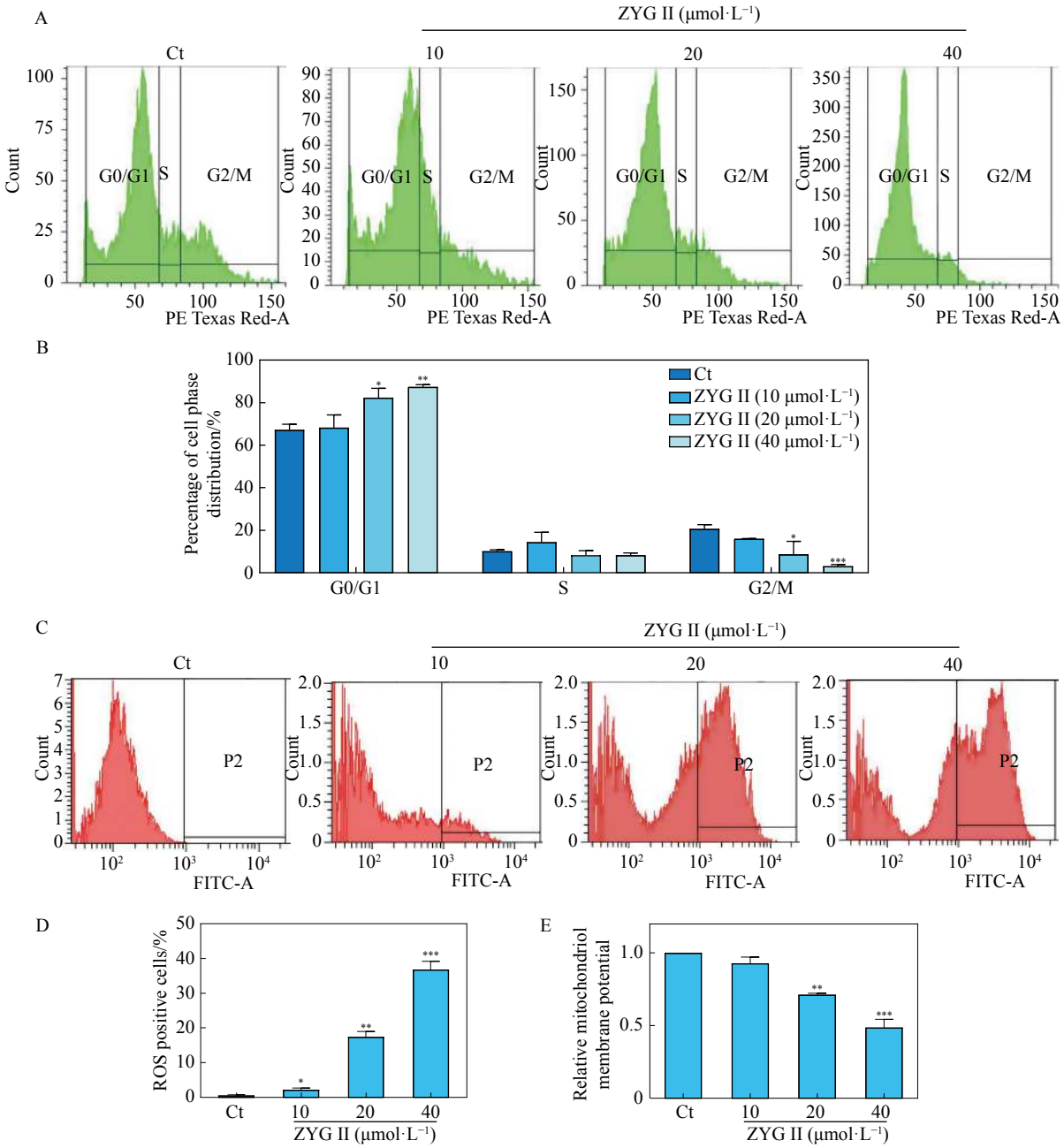

Fig. 3 ZYG II induces cell cycle arrest and oxidative stress in cancer cells. (A−B) HepG2 cells were treated with ZYG II (0, 10, 20, 40 μμmol·L^{-1}) for 24 h and the cell cycle distribution were determined by flow cytometry. (C−D) The percentage of ROS positive cells was obtained using flow cytometry. (E) Mitochondrial membrane potential (MMP) levels were determined as described in Materials and Methods. Representative images of flow cytometric analysis are shown and all results are expressed as mean ± SEM from three independent experiments. $^{*}P < 0.05$, $^{**}P < 0.01$, $^{***}P < 0.001$ *vs* control

6.10%, 82.30% ± 4.38%, and 87.35% ± 1.06%, respectively. At the same time, the population size of cells at S phase was not significantly affected by ZYG II.

Recent studies have shown that mitochondria is the main site of ROS production and is the central player in oxidative stress-related cell death. ROS facilitates oxidative damage to mitochondria mainly by oxidizing mitochondrial cardiolipin, DNA and functional proteins, thereby subsequently induces mitochondria-dependent apoptosis. The ROS levels were determined using flow cytometry assay after cells were treated with various concentration of ZYG II. As shown in Fig. 3C and 3D, the percentage of ROS positive cells were only 0.55% in control group, 2.20% in 10 μmol·L^{-1} ZYG II, and dramatically increased to 17.40% in 20 μmol·L^{-1} ZYG II and 36.75% in 40 μmol·L^{-1} ZYG II. The loss of mitochondria membrane potential (MMP) has been reported as an early event in response to excessive oxidative stress. Our data demonstrated that ZYG II led to significantly decreased

MMP in a dose dependent manner, which is closely associated with ZYG II-mediated substantial ROS accumulation (Fig. 3E).

Network construction and analysis

To explore the underlying mechanisms of ZYG II in treating digestive system cancers, we construct a ZYG II-digestive cancer protein-protein interaction network including 51 nodes and 278 edges, by combining the predicted targets of ZYG II derived from drug bank database and all targets of six digestive cancer based on experimental evidence extracted from comparative toxicogenomics database (Fig. 4A). Each node represented common targets for both ZYG II and digestive cancers. An edge represented an interaction between two nodes, which were weighted by the degree score calculated by the Cytoscape, as a relative importance of all edges in the network. The node size gets larger with in-

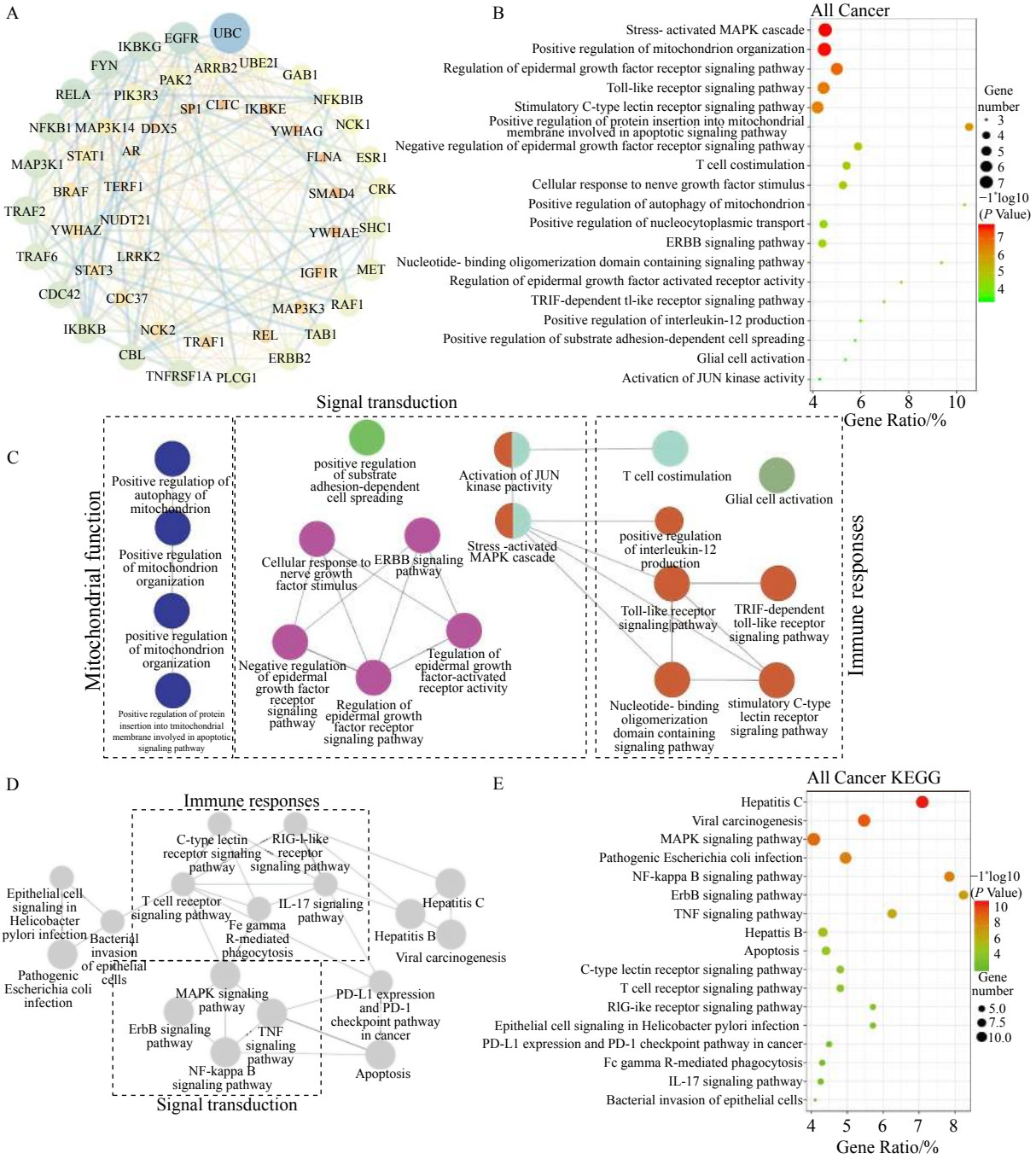

Fig. 4 Prediction of putative targets of ZYG II by network pharmacology. (A) Protein-protein interaction network of targets for ZYG II against digestive cancers. Each node represented common targets for both ZYG II and digestive cancers. (B, C) GO pathway enrichment analysis. (D, E) KEGG pathway enrichment analysis. (B, E) Bubble charts for GO and KEGG pathway enrichment analysis. (C, D) ClueGo analysis results representing the interaction between enriched GO and KEGG pathways

creased degree and the node color gets bright from blue to red with increased degree. Similarly, the edge color indicated the combine score of the correlation from bright to deep and the edge width was proportional to the correlation magnitude. The top ten selected targets, according to degree, are UBC, EGFR, IKBKG, FYN, RELA, KFKB1, MAP3K1, TRAF2, TRAF6 and CDC42, and a large number of targets have been confirmed to be closely related to the two proteins, NF-κB and EGFR, which mainly enriched in the molecular processes of inflammatory, cell migration and apoptosis.

After the selection of major targets, to interpret the potential mechanisms of ZYG II against cancer from a systematic level, we carried out GO enrichment analysis by importing selected 51 target genes into the CluGO, an app in cytoscape for pathway analysis, and enriched GO pathways are shown in Fig. 4B. Each point in the chart represents the enrichment level, the color corresponds to the adjusted *P*-value, and the size corresponds to the number of genes enriched. The top three pathways, according to the enrichment analysis, are stress-activated MAPK cascade, positive regulation of mitochondrion organization and regulation of epidermal growth factor receptor signaling pathway. In order to further understand the biological function of ZYG II in regulating cancer cell growth, these pathways are classified to establish a network visualization. As shown in the Fig. 4C, 19 pathways were select through GO enrichment analysis which could be divided into 3 sub-categories that related to mitochondria function, EGFR signaling and regulation of immune responses. The dark blue nodes, in the left panel of Fig. 4C, were involved in the regulation of mitochondrial function including positive regulation of autophagy of mitochondrion, positive regulation of protein insertion into mitochondrial membrane involved in apoptotic signaling pathway, which are potentially related to tumor inhibition. Pathways categorized in the middle panel are primarily associated with tyrosine protein kinase-mediated signaling pathways, including EGFR-mediated biological functions related to cell growth and survival. While pathways within the right panel are mainly consisted of signal pathways related to the regulation of immune responses, including toll-like receptor signaling pathway and T cell costimulation pathways, substantially suggested the plausible bioactivities of ZYG II in regulating cancer-related immune escape.

In KEGG enrichment analysis, as shown in the bubble chart (Fig. 4D), cancer growth-related pathways, such as MAPK signaling pathway, NF-kappa B signaling pathway, TNF signaling pathway and ErbB signaling pathway, are significantly enriched. And both the GO and KEGG pathway annotation suggested that EGFR signaling pathways and EGFR-related signal pathways were involved in the anti-cancer activities of ZYG II. As shown in Fig. 4D and 4E, 17 pathways were predicted. In addition to those pathways similar to GO enrichment analysis, others were found closely related to bacteria- and virus-mediated responses. Over the years, *in vitro* and *in vivo* experiments have revealed that hepatitis C, hepatitis B, contribute to the viral carcinogenesis of liver cancers. It is also noteworthy that *helicobacter* infection, pathogenic *E.coli* infection and bacteria invasion of epithelial cells are major risks of gastric and colorectal cancers. These results suggested that ZYG II are potential therapeutic agents against digestive cancers by regulating multiple signaling pathways.

Molecular Docking Simulation

The computational studies were performed to visualize the complex of ZYG II, Sorafenib with relative protein structures to further investigate the interaction between ZYG II and molecular targets predicated by network pharmacology analysis. Firstly, the EGFR kinase in complex with an ATP analog (PDB ID: 2GS6) was chosen as the binding template, since most of the current EGFR inhibitors are binding to the ATP pocket of EGFR (Fig. 5A—C). The docking scores of ZYG II towards the EGFR kinase target was 3.47 while the original ligand was 6.97, and the EGFR inhibitor Sorafenib obtained a score of 4.89. The binding modes of ZYG II, Sorafenib and the original ligand were predicted by the Surflex-Dock program. We found that ZYG II interacted with the EGFR kinase by forming hydrogen bonds with LYS721, THR766 and THR830 (Fig. 5B). The original ligand was found to form hydrogen bonds with LYS721, MET769, ASP776, ARG817, THR830 and ASP831, while the positive drug formed hydrogen bonds with MET769, ASP831, ARG817 Fig. 5A and C. The results implied that ZYG II had certain binding ability with the EGFR kinase, while the binding affinity was relatively weak when compared to the original ligand and Sorafenib. Additionally, the HER2 and VEGFR2 target was chosen to dock with ZYG II to further elucidate the plausible binding of ZYG II to other tyrosine kinases predicted by network pharmacology. However, the docking scores of ZYG II towards HER2 and VEGFR2 target were −3.50 and −24.69 respectively, while the total scores of the bound ligand towards these two proteins were 12.52 and 10.47. The docking results implied that ZYG II might not well bind with HER2 and VEGFR2 target. In conclusion, ZYG II might be a weak EGFR inhibitor which could bind with the ATP active pocket, and the supposition would be validated experimentally in further studies.

ZYG II inhibited EGFR signaling activation in HepG2 cells

To further elucidate the inhibitory interaction between ZYG II and EGFR, the phosphorylation of EGFR and downstream ERK activation were determined in HepG2 cells upon ZYG II treatment. Firstly, HepG2 cells were treated with 20 μmol·L^{-1} ZYG II for different time. As shown in Fig. 6A, the phosphorylation of EGFR was significantly inhibited by more than 8-fold as early as 1 hour after ZYG II challenge and then lasted for more than 4 hours. The phosphorylation of ERK1/2 was also rapidly reduced after ZYG II treatment, however, recovered more than 8 hours 1 hour later, indicating the involvement of other tyrosine kinases-dependent ERK activation in HepG2 cells which were not implicated by ZYG II. We further investigated the inhibitory effects of ZYG II at

different concentrations on EGFR signaling pathway and found that ZYG II abrogated the phosphorylation of both EGFR and ERK1/2 in a dose-related manner. (Fig. 6B). Tumor microenvironment with high levels of EGF is critical for the progressive growth of HCC. We further found that as low as 10 ng·mL^{-1} of EGF significantly induced the phosphorylation of EGFR and downstream of ERK1/2, which was dose-dependently blocked by ZYG II treatment. These results further confirmed that ZYG II is a potential EGFR inhibitor.

Synergistic anti-tumor effects of ZYG II and 5-FU on digestive system cancers

To further explore the potential clinical application of

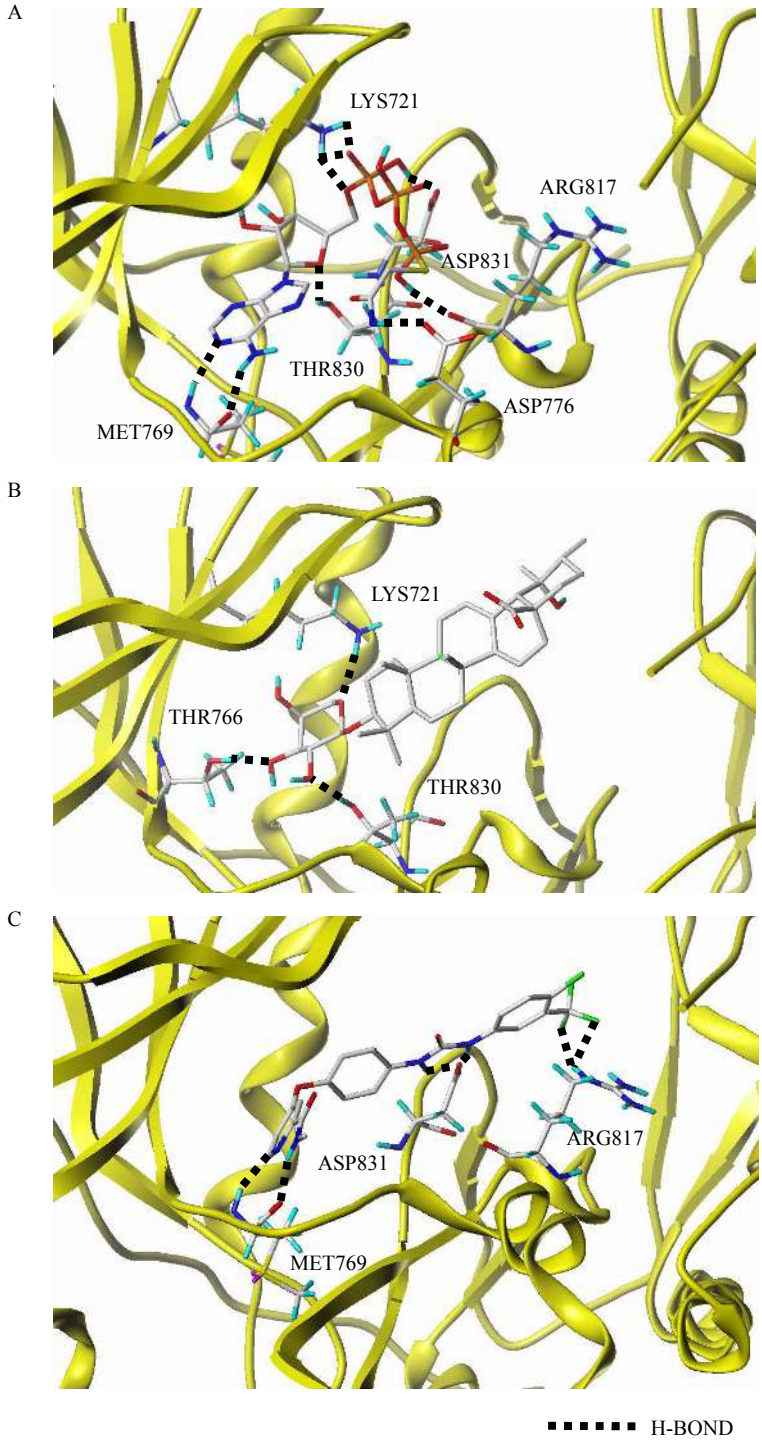

Fig. 5 Molecular Docking Simulation of ZYG II in complex of EGFR ATP binding pocket. Docking simulation was performed as described in the Materials and methods. (A−C) The docking results of the original ligand (A), ZYG II (B), and Sorafenib (C) in complex of EGFR kinase domain (2GS6)

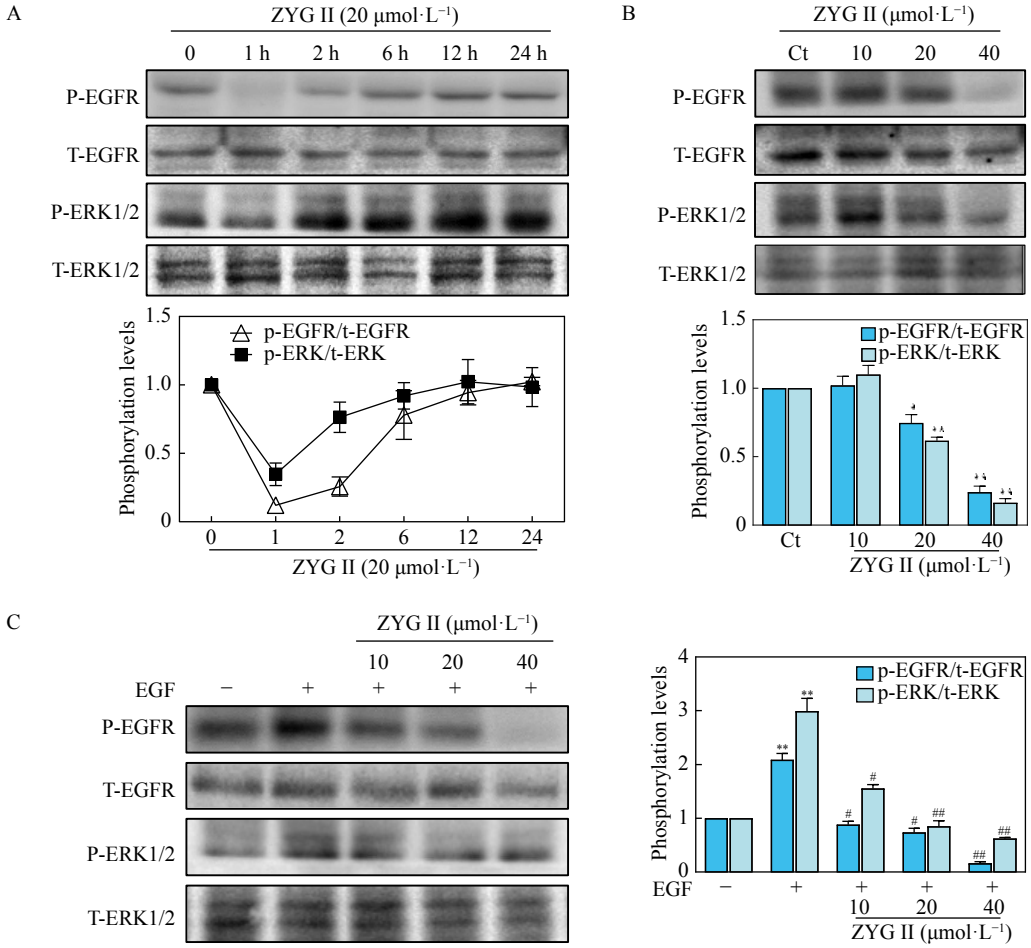

Fig. 6 ZYG II inhibits the activation of EGFR-ERK1/2 signaling pathway. (A) HepG2 cells were treated with 20 μmol·L^{-1} ZYG II for 1, 2, 6, 12, 24 h, and then the protein levels of Phosphorylated-EGFR (P-EGFR), Total-EGFR (T-EGFR), P-ERK1/2 and T-ERK1/2 were determined by western blot analysis. (B) HepG2 cells were treated with indicated concentrations of ZYG II for 2 h, and the protein levels of P-EGFR, T-EGFR, P-ERK1/2 and T-ERK1/2 were assessed by western blot analysis. (C) HepG2 cells were treated with indicated concentrations of ZYG II for 1 h. The cells were then treated with EGF (10 ng·mL^{-1}) for another hour. The protein levels of P-EGFR, T-EGFR, P-ERK1/2, T-ERK1/2 were determined by western blot analysis. The representative blot images are shown and the ratios of P-EGFR/T-EGFR and P-ERK1/2/T-ERK1/2 are shown. All results are expressed as mean ± SEM of three independent experiments. $^{*}P < 0.05$, $^{**}P < 0.01$, $^{***}P < 0.001$ *vs* control; $^{\#}P < 0.05$, $^{\#\#}P < 0.01$ *vs* EGF group

ZYG II, we next investigated whether ZYG II could cooperate with 5-FU, which has been used as the first-line drug for chemotherapeutic administration in cases of digestive cancer for several years to enhance its anti-cancer effects. First, we treated HepG2 cells with various concentrations of 5-FU and ZYG II for 24 hours as indicated in the figures, and the cell viability was assessed by CCK8 assay, and the synergism was assessed by constructing log(dose-reduction index) (log(DRI)), normalized isobologram and calculating combination index (CI) values using the Chou-Talalay method. Our results demonstrated that 5-FU inhibited HepG2 growth with a IC_{50} of around 100 μmol·L^{-1}. ZYG II dose-dependently sensitized HepG2 cells to 5-FU-induced cytotoxicity, as indicated by significantly reduced IC50 of 5-FU, about 12.5, 25, and 50 μmol·L^{-1}, with the presence of 10, 20 and 40 μmol·L^{-1} of ZYG II (Fig. 7A). Both the Fa-CI plot (Fig. 7B) and Normalized isobologram (Fig. 7C) demonstrated that the combination of ZYG II and 5-FU exerted synergistic anti-tumor effects against HepG2 cells growth as almost all data points located in the area of 0.5 < CI < 1 for Fa-CI plot and located in the triangles, respectively. Furthermore, as shown in Fig. 7D, ZYG II significantly potentiated the cytotoxicity of 5-FU in all tested digestive system cancers, except PANC-1, independent of their original sensitivities to 5-FU based chemotherapy.

Discussion

HCC is the second most prevalent form of malignant cancer in the world, while CRC is the third one, followed by pancreatic cancer, esophageal cancer and cholangiocarcinoma, which are all belong to digestive system neoplasms [16]. Although significant advancements in the combinational chemotherapy and targeted therapies and surgeries have been achieved, the recurrence and mortality rates of

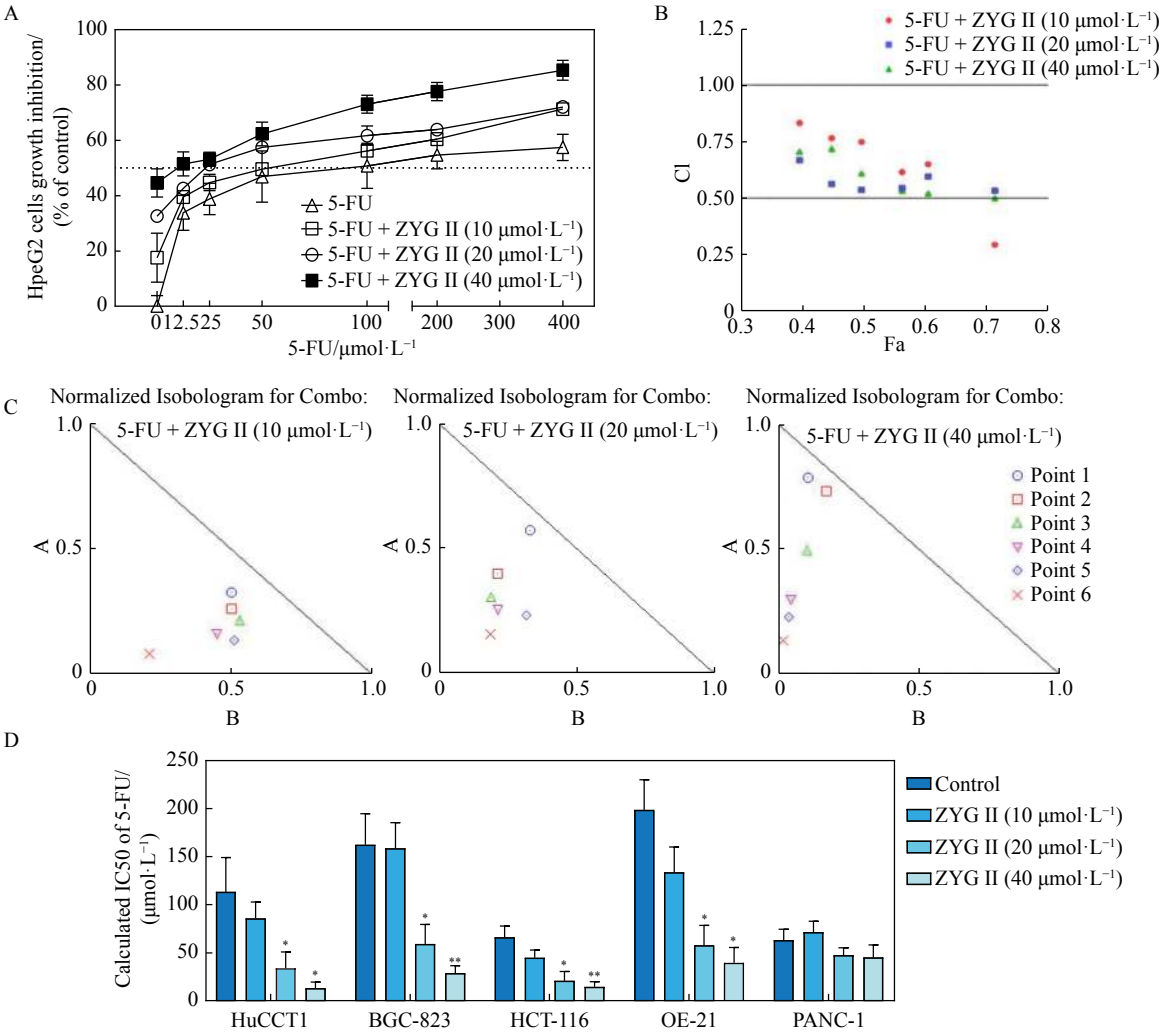

Fig. 7 ZYG II promotes the inhibitory effects of 5-FU on digestive cancer cells growth. (A) HepG2 cells were treated with various concentrations of 5-FU and ZYG II for 24 hours. At the end of experiment, the cell viability was assessed by CCK8 assay. (B and C) The synergism of 5-FU and ZYG II was assessed by constructing a Fa-CI plot, and a normalized isobologram graph using the Chou-Talalay equation in CompuSyn software. (B) Fa-CI plot of 5-FU and ZYG II, the X-axis indicates fraction affect (Fa) while the Y-axis indicates combination index (CI). Synergistic effect is defined by a CI below the line that CI < 1. (C) Normalized isobologram of 5-FU and ZYG II, the points in the triangle represent synergism effect of two drugs. (D) HuCCT1, BGC-823, HCT-116, OE-21, and PANC-1 cells were treated with different concentrations of 5-FU and ZYG II for 24 hours. The IC50 of 5-FU against different cancer cells were calculated and plotted. All results are expressed as mean ± SEM of three independent experiments. $^{*}P < 0.05$, $^{**}P < 0.01$ *vs* controltalic> < 0.01 *vs* control

these digestive cancer remains high. The intolerance to chemotherapies, limited responding rate to targeted therapies, multidrug resistance, and significant adverse effects brought obstacles to the treatment of digestive cancers and the improvement of life qualities of patients. Thus, continuous seeking of novel and tolerable anti-cancer agents is substantially requested. ZYG II is a natural compound derived from *Sanguisorba officinalis* L., a widely prescribed TCM herbal product, which has been safely used for over 2000 years with rare adverse effects reported. A plethora of evidence have demonstrated the anti-tumor effects of ZYG II. But our understanding of the mechanism underlying the anti-cancer effects of ZYG II is still fragmentary.

In the current study, our results strongly suggested that ZYG II significantly and dose-dependently inhibited the progressive growth of six digestive cancer cell lines, including HCC, CCA, GC, CC, EC and PC (Fig. 1). Among these cancers, HCC, CCA, GC and CC are more sensitive to ZYG II-induced growth arrest, when compared to EC and CC. Further studies indicated that ZYG II promoted HepG2 cells cell cycle arrest at G0/G1 phase which in turn induced Caspase-dependent apoptosis, as indicated by flow cytometry and western blot determination of the upregulation of apoptosis-related proteins, such as BAX, cleaved caspase-3 and cleaved PARP [17]. Apoptosis is a programmed cell death process mediated through the death receptor-mediated extrinsic pathway or the mitochondrial-mediated intrinsic pathway. We also demonstrated that ZYG II-mediated apoptosis is related to the

activation of oxidative stress, as indicated by increased intracellular ROS accumulation and mitochondrial membrane potential reduction. These results suggested that ZYG II induced mitochondria-mediated intrinsic apoptotic pathway but not death receptor-mediated extrinsic apoptotic pathway in HepG2 cells. Our results are in agreement with previous works reporting the pro-apoptotic effects of ZYG II against several other human cancer cell lines. Furthermore, we demonstrated that ZYG II significantly facilitated the cytotoxicity of 5-FU, a first-line chemotherapy and effectively reduced the required concentration of 5-FU to induce the death of cancer cells. Encouraged by these results, we aim to investigated the synergistic effects of ZYG II and other chemotherapies and targeted therapies to improve the efficacy and safety of these treatment by reducing doses. We will also be interested in evaluating the effects of ZYG II on reversing chemoresistance in the future.

Network pharmacology, a novel method which combined the system network analysis and the pharmacology, could clarify the synergistic effects and underlying mechanisms among the networks of compound-compound, compound-target and target-disease at molecular level, which shed novel lights to the interactions between compounds, genes, proteins and diseases. By applying network pharmacological approaches, we predicted putative targets of ZYG II. The PPI network suggested that UBC, EGFR, IKBKG are the most probable associated targets involved in the anti-cancer effects of ZYG II against digestive cancer. UBC, depending on the ubiquitination patterns on its Lys residues, have different functions including DNA repair, cell-cycle regulation, kinase modification, endocytosis, DNA-damage responses as well as in signaling processes leading to the activation of the transcription factor NF-kappa-B [18, 19]. IKBKG, the regulatory subunit of the IKK core complex which phosphorylates inhibitors of NF-kappa-B, is associated with DNA damage, host-virus interaction, and transcription regulation of inflammatory genes and has been well-characterized as a potential oncoprotein facilitating diseases progression in various cancers [20-22]. EGFR is a receptor tyrosine kinase binding ligands of the EGF family and activating several signaling cascades to convert extracellular cues into appropriate cellular responses, which is known to be critical for the survival and growth of different cancers, including HCC, CCA and other digestive cancers [23, 24]. The discovery of EGFR specific inhibitors or pan-tyrosine kinases inhibitors have attracted great attentions for the development of targeted therapy of cancers with epithelial origination. Several EGFR inhibitors, including sorafenib, Gefitinib and Osimertinib, have been approved for the treatment of HCC and other digestive cancers [25, 26]. Both GO and KEGG pathway enrichment analysis highlighted the involvement of regulating EGFR pathways and downstream signal transduction processes in ZYG II-mediated biological regulative functions. By performing Docking simulation, we suggested that ZYG II was a putative EGFR specific inhibitor with novel binding mode, yet low affinity and potency. Western blot analysis further confirmed that ZYG II time- and dose-dependently inhibited both basal and EGF-induced activation of EGFR signaling pathways and thus contributed to the growth inhibitory effects of ZYG II.

As mentioned above, immune responses-related pathways, such as T cell co-stimulation, and TCR activation, have also been suggested as potential targets of ZYG II. KEGG analysis further suggested the potential implication of ZYG II on pathogens-induced immune responses and following inflammation-related carcinogenesis. Until recently, cancer immunotherapy has become the state of art therapeutic strategies for the treatment of cancers. By activating innate and fine-tuning adaptive immune responses, immunotherapies bypasses immune escape mechanisms of cancer cells and exposure them to massive attacks mediated by cytotoxic T cells and other immune cells. KEGG analysis also implied that the putative targets of ZYG II were also implicated in the regulation of PD-1 and PD-L1-mediated immune escape. However, further experimental evidence is urgently required to fully characterized the immunoregulative effects of ZYG II and to elucidated whether these effects contributes to the anti-cancer properties of ZYG II.

In summary, the current study demonstrated that ZYG II effectively inhibited the progressive growth of various digestive system cancer cells, including HCC, CCA, GC, CC, GC and PC by inducing cell cycle arrest and activation of mitochondria-dependent apoptosisdet. Network pharmacology analysis and molecular biological validation suggested that the inhibition of EGFR signaling pathways are potentially involved in the anti-cancer effects of ZYG II. Further systemic evaluation of the anti-cancer activities *in vitro* and *in vivo* and characterization of underlying mechanism will promote the development of novel supplementary therapeutic strategies based on ZYG II for the treatment of digestive system cancers.

References

[1] Bray F, Ferlay J, Soerjomataram I, *et al*. Global cancer statistics 2018: GLOBOCAN estimates of incidence and mortality worldwide for 36 cancers in 185 countries [J]. *CA Cancer J Clin*, 2018, **68**(6): 394-424.

[2] Siegel RL, Miller KD, Jemal A. Cancer statistics, 2020 [J]. *CA Cancer J Clin*, 2020, **70**(1): 7-30.

[3] Chen X, Li B, Gao Y, *et al*. Saponins from *Sanguisorba officinalis* improve hematopoiesis by promoting survival through FAK and Erk1/2 activation and modulating cytokine production in bone marrow [J]. *Front Pharmacol*, 2017, **8**: 130.

[4] Liang J, Chen J, Tan Z, *et al*. Extracts of medicinal herb Sanguisorba officinalis inhibit the entry of human immunodeficiency virus type one [J]. *J Food Drug Anal*, 2013, **21**(4): S52-S58.

[5] Liu X, Cui Y, Yu Q, *et al*. Triterpenoids from Sanguisorba officinalis [J]. *Phytochemistry*, 2005, **66**(14): 1671-1679.

[6] Zhu LJ, Chen L, Bai CF, *et al*. A rapid and sensitive UHPLC-MS/MS method for the determination of ziyuglycoside I and its application in a preliminary pharmacokinetic study in healthy and leukopenic rats [J]. *Biomed Pharmacother*, 2020, **123**: 109756.

[7] Kim YH, Chung CB, Kim JG, *et al*. Anti-wrinkle activity of ziyuglycoside I isolated from a Sanguisorba officinalis root extract and its application as a cosmeceutical ingredient [J]. *Biosci Biotechnol Biochem*, 2008, **72**(2): 303-311.
[8] Zhu X, Wang K, Zhang K, *et al*. Ziyuglycoside I inhibits the proliferation of MDA-MB-231 breast carcinoma cells through inducing p53-mediated G2/M cell cycle arrest and intrinsic/extrinsic apoptosis [J]. *Int J Mol Sci*, 2016, **17**(11).
[9] Zhu AK, Zhou H, Xia JZ, *et al*. Ziyuglycoside II-induced apoptosis in human gastric carcinoma BGC-823 cells by regulating Bax/Bcl-2 expression and activating caspase-3 pathway [J]. *Braz J Med Biol Res*, 2013, **46**(8): 670-675.
[10] Nam SH, Lkhagvasuren K, Seo HW, *et al*. Antiangiogenic effects of ziyuglycoside II, a major active compound of *Sanguisorba officinalis* L. [J]. *Phytother Res*, 2017, **31**(9): 1449-1456.
[11] Lkhagvasuren K, Kim JK. Ziyuglycoside II induces caspases-dependent and caspases-independent apoptosis in human colon cancer cells [J]. *Toxicol In Vitro*, 2019, **59**: 255-262.
[12] Zhu X, Wang K, Zhang K, *et al*. Ziyuglycoside II inhibits the growth of human breast carcinoma MDA-MB-435 cells *via* cell cycle arrest and induction of apoptosis through the mitochondria dependent pathway [J]. *Int J Mol Sci*, 2013, **14**(9): 18041-18055.
[13] Zhu X, Wang K, Zhang K, *et al*. Ziyuglycoside II induces cell cycle arrest and apoptosis through activation of ROS/JNK pathway in human breast cancer cells [J]. *Toxicol Lett*, 2014, **227**(1): 65-73.
[14] Wang K, Zou P, Zhu X, *et al*. Ziyuglycoside II suppresses the aggressive phenotype of triple negative breast cancer cells through regulating Src/EGFR-dependent ITGB4/FAK signaling [J]. *Toxicol In Vitro*, 2019, **61**: 104653.
[15] Liao W, Fan L, Zheng Z, *et al*. Ziyuglycoside II exerts antiproliferative and antimetastasis effects on hepatocellular carcinoma cells [J]. *Anti-Cancer Drugs*, 2020, **31**(8): 819-827.
[16] Brenner H, Kloor M, Pox CP. Colorectal cancer [J]. *Lancet*, 2014, **383**(9927): 1490-1502.
[17] Fesik SW. Promoting apoptosis as a strategy for cancer drug discovery [J]. *Nat Rev Cancer*, 2005, **5**(11): 876-885.
[18] Huang F, Kirkpatrick D, Jiang X, *et al*. Differential regulation of EGF receptor internalization and degradation by multiubiquitination within the kinase domain [J]. *Mol Cell*, 2006, **21**(6): 737-748.
[19] Komander D. The emerging complexity of protein ubiquitination [J]. *Biochem Soc Trans*, 2009, **37**(Pt 5): 937-953.
[20] Zeng W, Xu M, Liu S, *et al*. Key role of Ubc5 and lysine-63 polyubiquitination in viral activation of IRF3 [J]. *Mol Cell*, 2009, **36**(2): 315-325.
[21] Zhou H, Wertz I, O'Rourke K, *et al*. Bcl10 activates the NF-kappaB pathway through ubiquitination of NEMO [J]. *Nature*, 2004, **427**(6970): 167-171.
[22] Luedde T, Schwabe RF. NF-kappaB in the liver-linking injury, fibrosis and hepatocellular carcinoma [J]. *Nat Rev Gastroenterol Hepatol*, 2011, **8**(2): 108-118.
[23] Runkle KB, Kharbanda A, Stypulkowski E, *et al*. Inhibition of DHHC20-mediated EGFR palmitoylation creates a dependence on EGFR signaling [J]. *Mol Cell*, 2016, **62**(3): 385-396.
[24] Chen WS, Lazar CS, Lund KA, *et al*. Functional independence of the epidermal growth factor receptor from a domain required for ligand-induced internalization and calcium regulation [J]. *Cell*, 1989, **59**(1): 33-43.
[25] Tanaka T, Ishiki H, Kubo E, *et al*. Is gefitinib combined with platinum-doublet chemotherapy a counterpart to osimertinib monotherapy in advanced EGFR-mutated non-small-cell lung cancer in the first-line setting? [J]. *J Clin Oncol*, 2020, **38**(8): 843-844.
[26] Cho JH, Lim SH, An HJ, *et al*. Osimertinib for patients with non-small-cell lung cancer harboring uncommon EGFR mutations: a multicenter, open-label, phase II trial (KCSG-LU15-09) [J]. *J Clin Oncol*, 2020, **38**(5): 488-495.

Cite this article as: ZHONG Ying, LI Xiao-Yu, ZHOU Fei, CAI Ya-Jie, SUN Rong, LIU Run-Ping. Ziyuglycoside II inhibits the growth of digestive system cancer cells through multiple mechanisms [J]. *Chin J Nat Med*, 2021, **19**(5): 351-363.

Dr. SUN Rong is a professor of medicine at Shandong University and the Second Hospital of Shandong University, Tai-Shan Scholar of Traditional Chinese medicine (TCM), and the vice chairman of the Committee on Toxicology and Safety Evaluation of Chinese Materia Medica of China Pharmaceutical Society Geriatric Pharmacy. She has dedicated to the translational researches of TCM to improve efficacy and safety. She focused on not only the re-evaluation and development of patented and marketed TCM drugs but also the discovery of novel drug candidates for the treatment of severe chronic diseases, including cancers, from the diverse library of natural products derived from herbal medicines. She has completed more than 50 provincial and national projects, including 973 and 863 plans, obtained 11 authorized invention patents, and published more than 100 TCM-related papers in the past 5 years, including 12 articles indexed in SCI, 3 books as chief editor, and 7 books as associate editor. Based on her accomplishments, she was awarded “Distinguished Individuals in TCM” in May 2009 and “Shandong Province TCM Outstanding Contribution Award” in November 2020. As the first accomplice, she also won 2 first prizes and 2 second prizes of Science and Technology Progress in Shandong province.